34th Annual International Conference of the IEEE EMBS
San Diego, California USA, 28 August - 1 September, 2012

Heating characteristics with a re-entrant type applicator in consideration of tissue blood flow rate

T. Ishimori[1], Y. Ishihara[2]

Abstract— **We have proposed the heating system based on a re-entrant cavity that can heat a localized deep region in a living body noninvasively. This system is superior in a local heating characteristic. However, when the living body was treated as a heating object during thermotherapy (hyperthermia), the effect of blood flow changes on a heating characteristic has to be examined. The purpose of this study was to establish the quantitative evaluation method of heating characteristics for a re-entrant type applicator. The numerical analyses by using three-dimensional finite element method in consideration of a blood flow and fundamental experiments with prototype system were carried out. Since the difference of numerical analyses and experiments was as small as about 4.2 [%] by evaluation with full width at half maximum (FWHM), the validity of this numerical analysis was confirmed.**

I. Introduction

In recent years, the thermotherapy (hyperthermia) attracts attention as a physical therapy of cancer. In hyperthermia, it is necessary to heat cancer at around 43 °C locally to treat it effectively. We have proposed the heating system based on a re-entrant cavity that can heat a localized deep region in a living body non-invasively [1]. This heating system consists of a resonator with an inner cylinder called as a re-entrant that is attached to the upper and lower parts of the cylindrical cavity. The electromagnetic field is formed at the re-entrant gap intensively since the standing wave of the electromagnetic field is excited in a re-entrant cavity. As a result, a lesion inside a living body is heated effectively when it is inserted in this gap [2], [3]. Until now, the validity of this system has been confirmed and the small size re-entrant type applicator has been developed to heat a tumor located in a head and neck.

On the other hand, it is necessary to take into consideration the inhomogeneous temperature distribution in a living body as the localized heating characteristics are improved. This is because the local reaction of the living body by the local heating occurs. For example, normal tissue has an about 2 – 10 times blood flow compared with a tumor tissue [4]-[6]. Furthermore, in contrast to the blood flow in normal tissue increasing due to vasodilatation, that in tumor tissue hardly changes. As results, even if the same heat dose is given, temperature change in each living tissue differs remarkably. Despite this, a cooling effect due to the blood flow was not taken into consideration in our previous study for a re-entrant type system. Then, the purpose of this study is the quantitative evaluation of the heating characteristics for a re-entrant type applicator. The numerical analyses by using three-dimensional finite element method in consideration of a blood flow, and fundamental experiments with prototype heating system are carried out.

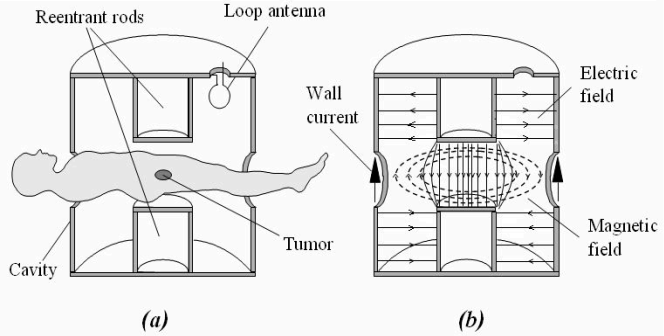

Figure 1. Overview of the heating system using reentrant resonant cavity. (a) Cross-section of the reentrant resonant cavity. (b) Electromagnetic distribution inside the reentrant resonant cavity in the lowest order mode.

II. Principle

The electromagnetic distribution inside the re-entrant resonant cavity is governed by the Helmholtz's equation as expressed as equation (1). An electromagnetic distribution is generated inside the resonant cavity as the lowest resonance mode, and shown in Fig. 1 (b).

$$\begin{aligned} &\nabla^2 E + k^2 E = 0 \\ &\nabla^2 H + k^2 H = 0 \\ &k^2 = \omega^2 \varepsilon \mu \end{aligned} \tag{1}$$

Here, ω represents angular frequency (rad/s), ε represents dielectric constant (F/m), and μ represents permeability (H/m). With this heating system, a standing wave is generated between the re-entrant electrodes, and the electric field strength is the strongest at the center of these electrodes, and decreases rapidly in the direction of the radius. In addition, the electric field between the re-entrant electrodes along the longitudinal axis is distributed as a sine function form, and therefore the electric field at the center of the electrode will be strong compared to the neighborhood of the electrode. This is different in the case of a conventional RF

1.Graduate school of Mechanical Engineering, Meiji University, 1-1-1 Higashi-mita, Tama-ku, Kawasaki 214-8571, Japan (corresponding author to provide phone: +81-44-934-7416; fax: +81-44-934-7907; e-mail: ce12010@meiji.ac.jp)
2.Department of Science and Engineering, Meiji University, 1-1-1 Higashi-mita, Tama-ku, Kawasaki 214-8571, Japan (corresponding author to provide phone: +81-44-934-7416; fax: +81-44-934-7907; e-mail: y_ishr@meiji.ac.jp)

capacitive heating system. Thus, by placing the target region for treatment between the re-entrant electrodes, deep lesions of a living body can be heated locally, non-invasively, and without contact.

In order to calculate temperature distribution in consideration of a blood flow, the bio-heat transfer equation expressed with the following equation is used [7].

$$\rho c \frac{\partial T}{\partial t} = div(\kappa \quad gradT) + W_h + \rho_b c_b f(T_b - T) \qquad (2)$$

where ρ and ρ_b [kg/m^3], density of tissue and blood, respectively; c and c_b [J/ (kg・K)], the specific heat of tissue and blood, respectively; T [K], temperature; T_b [K], temperature of blood; f [m^3/s], blood flow rate; κ [W/(m・K)], thermal conductivity; and W_h [W/kg], absorbed thermal power density due to the heat source of RF field. In this study, other parameters such as the metabolism effect are neglected.

III. METHODS

A. Numerical analysis

First, the electromagnetic field distribution in an applicator (the height of a re-entrant type cavity resonator: 950 [mm], the outside cylinder: 350 [mm], the gap length: 400 [mm], the inner cylinder: 50 [mm]) shown in Fig. 2 was calculated by the finite element method (FEM). A phantom model of cylinder type with size of 160 × 150 [mm] was used. This model was made equivalent to the phantom used in the after mentioned experiments.

Next, the temperature distribution inside the phantom was also calculated by the FEM. In order to consider the blood flow, the inner region (diameter of 60 [mm], height of 150 [mm]) of this phantom was simulated as a tumor tissue without blood flow, and the outer region was simulated as the normal tissues with blood flow of 600 [ml] circulated every one minute (Fig. 3). The other conditions were shown in Table I - III.

In this study, the heating characteristics along each axis of the r-direction and the z-direction defined as Fig. 2 were evaluated with the full width at half maximum (FWHM) after normalizing temperature distribution.

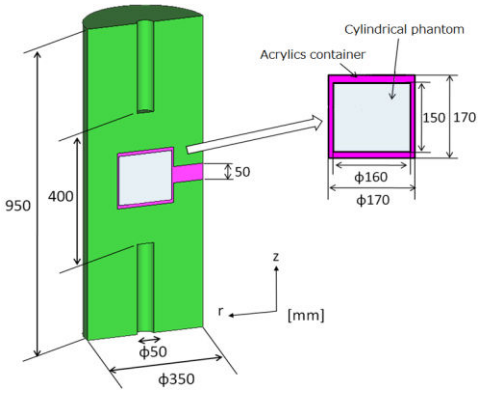

Figure 2. Numerical ayalysis model

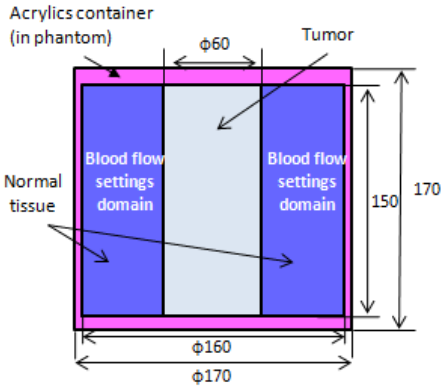

Figure 3. Phantom model simulated blood flow

TABLE I. ELECTROMAGNETIC PROPERTIES OF FEM MODEL

	Air	Phantom	Acrylic
Relative permeability	1	1	1
Relative permittivity	1	63	2.7
Electrical conductivity [S/m]	0	0.47	1×10^{-16}

TABLE II. HEAT TRANSFER PROPERTIES OF FEM MODEL

	Phantom	Acrylic
Thermal conductivity [W/(m・K)]	0.55	0.2
Specific heat [J/(kg・K)]	4200	1470
Volume density [kg/m^3]	980	1190

TABLE III. ANALYSIS CONDITIONS

	Without blood flow	With blood flow
Initial temperature [℃]	37.0	37.0
Atmosphere temperature [℃]	37.0	37.0
Blood flow [ml/min]	0	600
Heating time [min]	20	20

B. Heating experiment

The heating experiment was performed using an applicator with the same size as the numerical analysis. The block diagram of the heating system was shown in Fig. 4. This prototype system consists of a resonator, an RF amplifier, an RF oscillator and a temperature control pump. The pump and the acrylics container including an agar phantom were connected, and the heating was carried out during the circulation of the water with the constant temperature. The experimental conditions were shown in Table IV. The phantom in consideration of a blood flow was shown in Fig. 5. The shape of this phantom was cylindrical (diameter: 160 [mm], height: 150 [mm]), and many holes with diameter of 2 [mm] at every 10 [mm] intervals in the outer region (a larger region than 60 [mm] in diameters) were opened to simulate the blood vessels in the normal tissue. In contrast to this, the inner region smaller than 60 [mm] in diameters was simulated as a tumor tissue with few blood flows (without a hole).

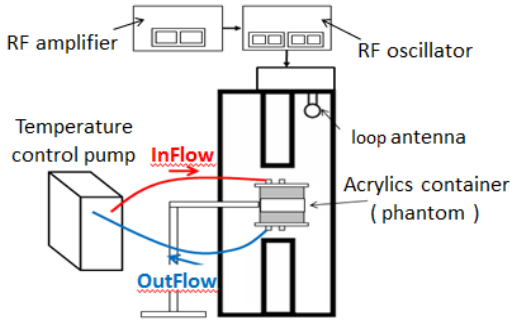

Figure 4. Heating system

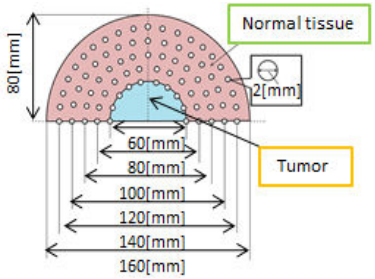

Figure 5. Blood flow phantom

TABLE IV. EXPERIMENTAL CONDITIONS

	Without blood flow	With blood flow
Apply electric power [W]	40	40
Resonance frequency [MHz]	230.51	230.07
Initial temperature [℃]	24.3	30.3
Atmosphere temperature [℃]	25.0	25.0
Blood flow [ml/min]	0	600

IV. RESULTS

The temperature distributions at the central section of the phantom obtained from the numerical analysis and the experiment were shown in Fig. 6 when the SAR in the phantom was set at 20 W/kg. The normalized temperature distributions were shown in Fig. 7. From the results of the numerical analysis, the heating region of r- direction was about 53 [mm], and was decreased about 30 [%] for the numerical simulation and 24 [%] for the experiment shown in Fig. 7 compared with each case without a blood flow. Experimental values agreed well with the numerical analysis results with the error of about 4.2 [%] by evaluation of FWHM. However, in particular, there were some differences along r-direction shown in Fig. 7 (a).

V. DISCUSSION

As the result shown in Fig. 7 (a), the numerical analysis in consideration of a blood flow indicated the difference at the larger regions than 40 mm from the phantom's center compared with the experiment. This error corresponded to about 0.15 with the normalized temperature scale. This reason was because the blood vessel models in a phantom differ in the numerical analysis and the experiment. In the FEM model, the averaged blood flow was taken into consideration at the outside region as the simulated normal tissue. Specifically, it means that the blood vessel was considered in each node of this FEM model as shown in the conceptual diagram of Fig. 8 (a). Therefore, it is thought that the blood vessel in the FEM model was simulating comparatively well the capillary vessel in an actual living tissue.

On the other hand, the blood vessel model in the phantom used in an experiment was shown in Fig. 8 (b). As mentioned above, the blood vessel was simulated as many holes at 10 [mm] intervals with the diameter of 2 [mm]. Then the water equivalent to the volume of tissue blood flow was continuously circulated by using the temperature controlled pump. However, since the diameter of a blood vessel and the density in tissue differed from numerical analysis, it was thought that the above-mentioned difference occurred.

In the future, in order to evaluate correctly a heating characteristic for the re-entrant applicator under various blood flow conditions, it is necessary to clarify validity of this numerical analysis. Then, although it differed from the capillary model in a living tissue, numerical analysis was carried out using the same blood vessel model (Fig. 8 (b)) as an experimental condition.

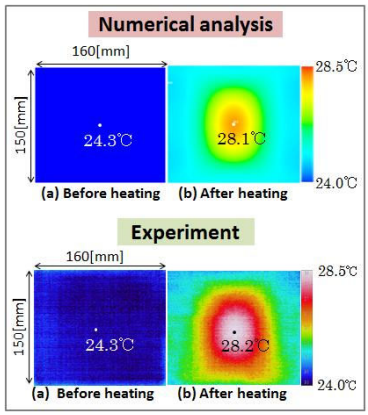

(A) Without blood flow

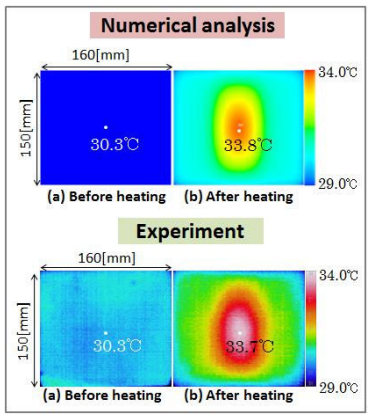

(B) With blood flow

Figure 6. Temperature distribution at the central section of the phantom

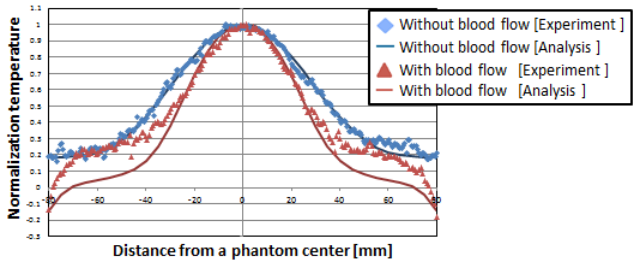

(a) r- direction

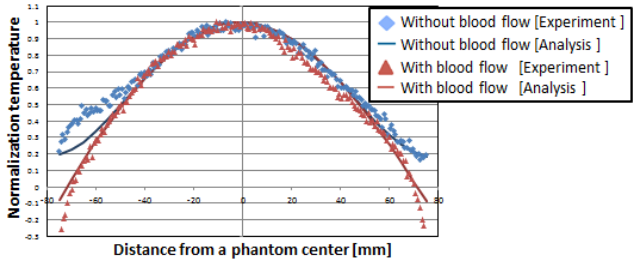

(b) z- direction

Figure 7. Normalized temperature distribution

The normalized temperature distribution at the central section of the phantom with large blood vessels was shown in Fig. 9. The difference of the temperature distribution between numerical analysis with large blood vessels and the experiment decreased shown in Fig. 9 (a). Both error was less than about 0.16 in a normalized temperature scale, and became smaller than the error in the case of a capillary vessel model. On the other hand, the temperature distribution in this experiment indicated left-right asymmetry, and the error became large at the left end of the phantom. This was considered that the volume of the water which flows into a left end phantom decreased. In this experiment system, since it was difficult to throw same volume of water in each hole of the phantom, the improvement of a phantom was required.

From these results, it was shown that the evaluation of heating characteristic in consideration of a blood flow is feasible by using this numerical analysis method. In the future, the heating region achieved by a re-entrant type applicator will be clarified against the sizes of a blood flow and a tumor using this method with a capillary vessel model. Furthermore, it is necessary to devise the phantom which realizes a capillary vessel model and to also perform experimental verification.

VI. Conclusion

In this study, the localized heating characteristics in consideration of tissue blood flow were evaluated by the numerical analysis and the experiments. As a result compared with the heating regions between the numerical analysis and the experiment, both differences were 4.2%. Then, it was shown that the evaluation of heating characteristic in consideration of a blood flow is feasible by using this numerical analysis method. However, the need for improvement was suggested about the blood vessel model in the phantom used in the experiment.

Acknowledgment

This study was supported by the Industrial Technology Research Grant Program from the New Energy and Industrial Technology Development Organization (NEDO) of Japan.

References

[1] Y. Ishihara, Y. Gotanda, N. Wadamori, J. Matsuda, Hyperthermia applicator based on a reentrant cavity for localized head and neck tumors, Rev. Sci. Inst., Vol. 78, pp. 024301-1－024301-8, 2007.

[2] J. Matsuda, K. Kato, Y. Saito, The application of a re-entrant type resonant cavity applicator to deep and concentrated hyperthermia, Jpn. J. Hyperthermia Oncol., Vol. 4, No. 2, pp. 111-118, 1988.

[3] Y. Saito, J. Matsuda, K. Kato, Characteristics of re-entrant type cavity applicator for hyperthermia, Jpn. J. Hyperthermia Oncol., Vol. 7, No. 1, pp. 42-52, 1991.

[4] Y. Yang, B.K. Lewis, S. Xu, A. Frank, J.H. Duyn, Quantitative CBF Mapping on Brain Tumor Patients Using Multislice Perfusion Imaging with Pulsed Arterial Spin-Labeling, The Institute of Electronics, Information and Communication Engineers, B, Vol. J85-B, No. 5, pp. 597-608, 2002.

[5] Grinev Iqor, Measurement of Regional Blood Flow by Laser Doppler Flowmetry in Rat Normal Brain and Glioma During Interstitial Hyperthermia, Niigata medical journal, Vol. 119, No. 5, pp. 294-302, 2005.

[6] Afonso C.Silva, Seong-Gi Kim, Michael Garwood, Imaging Blood Flow in Brain Tumors Using Arterial Spin Labeling, Magnetic Resonance in Medicine Vol. 44, pp. 169-173, 2000.

[7] Pennes, H.H, Analysis of Tissue and Arterial Blood Temperatures in the Resting Human Forearm, Journal of Applied Physiology, Vol.1, 1948, pp. 93-122.

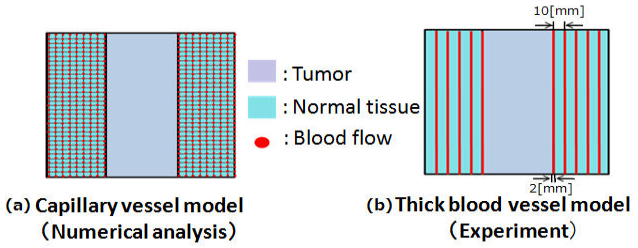

Figure 8. Blood flow conditions

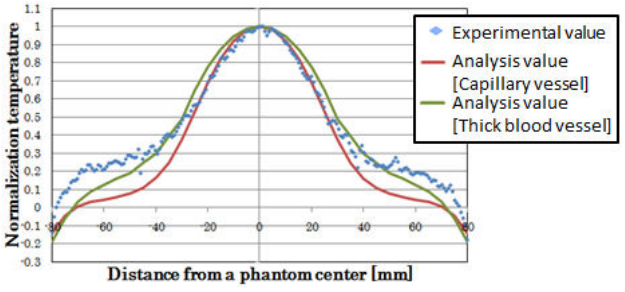

(a) r-direction

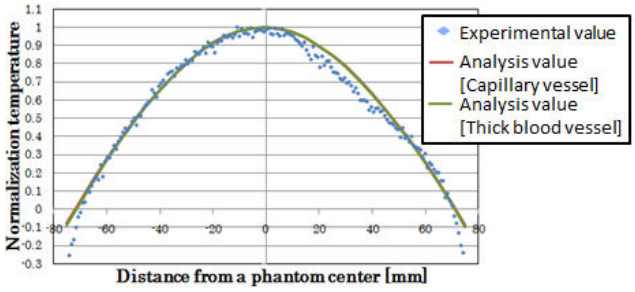

(b) z-direction

Figure 9. Phantom central sectional normalization temperature distribution